Metal ion recognition and molecular templating in self-assembled monolayers of cyclic and acyclic polyethers

Maria Ángeles Herranz, Barbara Colonna, and Luis Echegoyen*

Department of Chemistry, Clemson University, Clemson, SC 29634

Edited by Jack Halpern, University of Chicago, Chicago, IL, and approved February 6, 2002 (received for review December 10, 2001)

Our recent work with cyclic and acyclic polyether self-assembled monolayers (SAMs) on gold is presented. A series of dithia-crown-tetrathiafulvalene derivatives with one or two disulfide groups has been prepared, and their SAMs on gold have been characterized by electrochemistry and by reflection–absorption infrared spectroscopy. These SAMs are extremely stable on repeated electrochemical potential scans and can selectively recognize alkali metal ions. Acyclic polyether derivatives can also self-assemble on gold to yield selective metal ion recognition domains. Impedance spectroscopy data for these SAMs fit the Langmuir isotherm and allow the determination of ion association constants. Some of the SAMs prepared with new acyclic polyether derivatives are able to detect potassium cations selectively when templated in their presence. These structures are believed to be a consequence of ion ''imprinting'' during the process of SAM formation.

The easy preparation, stability, and versatility of self-assembled monolayers (SAMs) has resulted in considerable activity in this field since the first publication by Nuzzo and Allara (1). Molecular recognition is especially relevant on surfaces because it allows the control of the exchange of signals, structures, and energy through the interfaces (2–4). SAMs allow the introduction of functional groups in the adsorbates, thus offering a powerful way to develop systems that have applications as sensors, devices, and switches (5). Some recent articles have reported surface structures with hydrophobic and hydrophilic properties arranged in nano-strips and honeycomb or homogeneous structures (6), whereas others have detected photo and electrochemical conversion of cis to trans forms within the SAM (7). Other examples have shown the formation of chiral imprinted sites (8). SAM structures have also been prepared for the recognition and sensing of metal ions (9), some of which are electrochemically active (10–18).

Relatively recently, Reinhoudt *et al.* (19–22) and Bryce *et al.* (23, 24) reported, almost simultaneously, the incorporation of crown-ether groups into SAMs and their use as potential metal ion sensors. The Reinhoudt group used electrochemical impedance spectroscopy (EIS) for SAM characterization and to study the ion recognition processes (19–22). This technique enables the detection of interfacial ion recognition phenomena when both guest ion and host monolayer are electrochemically inactive, by detecting changes of the charge-transfer resistance induced by metal ion binding (see Fig. 1*a*; refs. 25 and 26). The report by Bryce *et al.* (23, 24) described SAMs of crown-annelated tetrathiafulvalene (TTF) derivatives, which showed, by cyclic voltammetry (CV), a redox potential shift of the electroactive, surface-confined, crown-TTF group on ion complexation (23, 24). The first TTF-crown SAMs reported by this group were apparently unstable after several electrochemical scans (23). However, in a subsequent report they demonstrated that the stability and electrochemical behavior of the SAMs can be improved by the presence of an additional space-filling alkyl chain (24). Thus, direct detection of ion binding may be achieved by monitoring the redox potential shift of a surface-confined electroactive group such as TTF, which is in close proximity to the ion host. This is illustrated in Fig. 1*b* with an example from our own recent work, described below. Both of these methods have been used to detect surface ion binding for the compounds described here.

In addition to using EIS and CV to detect ion binding by crown bearing SAMs, we decided to probe the effect of the degree of covalent preorganization of the host on ion binding and selectivity (27). The compounds chosen (see Fig. 2) range from the relatively rigid dithia-crown ethers (highly preorganized) to the very floppy podands (exhibiting essentially no preorganization). The structure in the middle possesses intermediate rigidity due to the presence of the naphthyl group.

Here we report the results obtained for bis-thioctic ester derivatives of crown ether annelated TTFs, similar to structure *a* in Fig. 2. We show how they form remarkably stable SAMs with surface-confined electrochemistry, and how they are able to selectively detect alkali metal ion binding (28, 29). We also introduce the use of acyclic oligoethyleneglycols (podands), such as structure *c* in Fig. 2, as surface binding domains (30, 31). SAMs of these compounds grown by themselves show ion binding properties and selectivities similar to those exhibited by 15-crown-5 or 18-crown-6 in aqueous solution (32), when the number of $(—CH_2—CH_2—O—)_n$ units in the podand is five or six, respectively, making them potentially useful monolayer sensors (32).

While molecular recognition sites can be introduced in a SAM as preformed entities (such as the cyclic and acyclic crown ethers described above), they can also form via self-assembly of non-organized groups under the action of molecular imprinting. The latter means that the growth of the SAM occurs in the presence of an appropriate analyte that templates the aggregation of groups that collectively form the recognition motif (33). This strategy was used initially by Chailapakul and Crooks in the assembly process of two-component SAMs, where one compound was much shorter than the other. Defects could be created in the longer monolayer, allowing these SAMs to respond selectively to different types of redox-active species (34, 35). In recent years Willner *et al.* (36) and Wolfbeis *et al.* (37) have also used this methodology to generate binding sites for organic substrates at the surface of modified electrodes. Surprisingly, no examples of SAM formation involving metal ion templates had been reported until our recent work (38, 39). In this article, we also report the preparation and the electrochemical investigations of potassium-imprinted SAMs on gold, using structures similar to *c* in Fig. 2, which selectively detect K^+ but not Na^+.

Materials and Methods

Materials. The gold substrates for the cyclic voltammetric and impedance experiments were prepared by annealing the tip of a gold wire (99.999%, 0.5 mm diameter, Alfa Ashe) in a gas–oxygen flame. Subsequently, the hot gold bead was cooled down in deionized water (Barnstead Nanopure, 18 MΩ). The quality of the

This paper was submitted directly (Track II) to the PNAS office.

Abbreviations: SAM, self-assembled monolayer; TTF, tetrathiafulvalene; RAIR, reflection–absorption infrared spectroscopy; CV, cyclic voltammetry; OEG, oligo(ethyleneglycols).

*To whom reprint requests should be addressed. E-mail: luis@clemson.edu.

 www.pnas.org/cgi/doi/10.1073/pnas.072658799

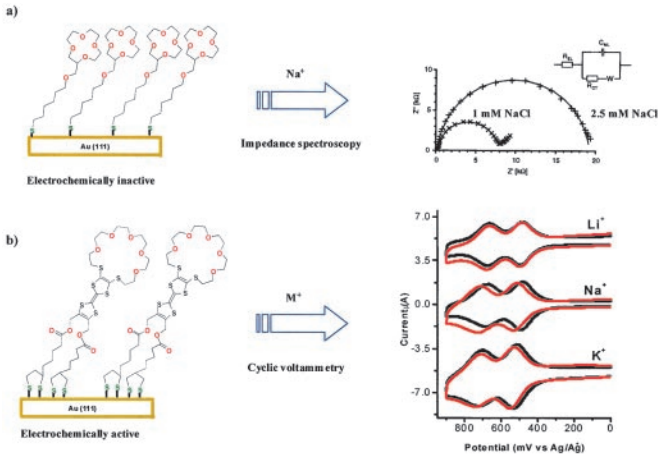

Fig. 1. Comparison between electrochemically inactive (*a*; ref. 11) or active (*b*; ref. 29) SAMs and the methodology used for their detection.

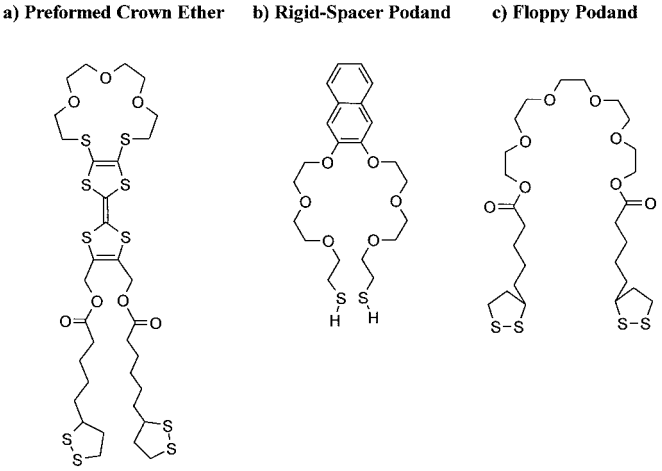

Fig. 2. Structures representing different degrees of preorganization of ion binding.

electrode surface was checked by observing the reversible redox response of $Ru(NH_3)_6^{3+/2+}$ in aqueous KCl. Electrodes not exhibiting the reversible response of the redox couple with peak to peak separation ≈60 mV were discarded. The geometric area of the electrode (typically 0.2–0.4 cm^2) was obtained from the slope of a linear plot of the cathodic current versus (scan rate)$^{1/2}$ for the reversible reduction of the above-mentioned redox probe, taking 7.5×10^{-6} cm^2/s as the diffusion coefficient, and knowing the exact concentration from the mass (40). The gold substrates for reflection–absorption infrared spectroscopy (RAIR) are prepared by vacuum deposition of gold (at a pressure of $\approx 10^{-7}$ Torr) on glass microslides coated with 3 mercaptotrimethoxysilane for better adhesion (41).

Preparation of Monolayers. In a typical experiment, a monolayer was grown by dipping a freshly prepared gold bead electrode in a 1–5 mM deaerated solution of EtOH, EtOH/H_2O, or CH_2Cl_2 (containing the appropriate disulfide in mM concentrations, in the case of TTF monolayers) of the respective compound for periods between 24 and 48 h. The substrates were removed, rinsed with the appropriate solvent, and dried in a stream of Ar. The monolayers grown in the presence of cations were prepared analogously in a solution (1–5 mM) of the corresponding solvent (EtOH, EtOH/H_2O, or CH_2Cl_2) that additionally contained 0.1 M of the desired salt and were dipped for the same length of time as in case of the plain monolayer. The electrodes were initially rinsed with deionized water followed by the respective solvent and then dried in a flow of Ar.

Electrochemical Measurements. Impedance and cyclic voltammetric measurements were performed using a three-electrode cell comprising a gold bead as the working electrode, a coiled platinum wire as the counter electrode, and an Ag/AgCl (from Bioanalytical Systems, West Lafayette, IN) as the reference electrode. Both electrochemical experiments were carried out with a Bioanalytical Systems 100-W electrochemical workstation interfaced with a personal computer. Impedance measurements were performed at the formal potential of the redox couple, and readings were taken at ten discrete frequencies per decade. The formal redox potential [$E_{1/2} = (E_p^c + E_p^a)/2$], where [$Ru(NH_3)_6^{3+}$] = [$Ru(NH_3)_6^{2+}$] was determined from cyclic voltammetry. The frequency range used was 1 KHz to 0.1 Hz with an alternating current (AC) amplitude of 5 mV. Impedance analysis was carried out using the commercially available program EQUIVALENT CIRCUIT written by B. A. Boukamp (University of Twente, The Netherlands), which determines the parameters of the assumed equivalent circuit by a nonlinear least-squares fit (42). All experiments were carried out at room temperature (25 ± 0.1°C) with tetraethylammoniumchloride as supporting electrolyte.

Infrared Spectroscopy. The reflection–absorption (RA) spectra were recorded on a Perkin–Elmer 2000 Fourier transform (FT)-IR spectrophotometer, equipped with a grazing angle (80°) infrared reflection accessory and a ZnSe wiregrid polarizer from International Crystal Laboratory. The spectra were recorded with a liquid-nitrogen-cooled MCT detector and the measurement chamber was continuously purged with nitrogen gas during the measurements. Typically 1,000 scans with 4 cm^{-1} resolution were performed to get the average spectra. A clean and freshly prepared gold plate was used to record the reference spectra. The RAIRS are reported as $-\log(R/R_0)$, where R and R_0 are the reflectivities of the sample and reference, respectively.

The transmission infrared spectra of the compound was recorded as a thin film prepared by putting a drop of the solution of the compound on a quartz cell and then evaporating it with a flow of Ar in the same spectrometer using 500 scans with 4 cm^{-1} resolution.

Results and Discussion

Dithia-Crown-Ether Annelated Tetrathiafulvalene Disulfides. In 1999, Fujihara *et al.* (43) reported a TTF compound containing four thiol groups, which formed very stable SAMs on gold electrodes after repeated voltammetric cycles. The use of such multiple anchoring sites provides very strong adherence of the compound to the metal surface, especially if the sulfur atoms are present within the same ring structure, in which case they exhibit an additional chelate effect (44). For these reasons, the use of thioctic acid derivatives as anchoring groups for SAMs has recently received considerable attention (45). In addition, the commercial availability of thioctic acid (1,2-dithiolane-3-valeric acid) stimulated us to prepare compounds **1a**–**1d** and **2a** and **2b** shown in Fig. 3.

Compounds **1a**–**1d** were directly synthesized in high yield by reacting the corresponding bis-alcohols with thioctic acid in the presence of 1,3-dicyclohexylcarbodiimide (DCC) and 4-(dimethylamino) pyridine (DMAP), using CH_2Cl_2 as solvent (10–18). The corresponding crown-annelated TTF bis-alcohol precursors were prepared in reasonable yields following a modification of the literature procedures (28, 29, 46). The mono-alcohol precursors to synthesize **2a** and **2b** were obtained by controlled reduction of the ester group of diester EDT-TTF (47). This direct coupling reaction to prepare TTF disulfides is general, straightforward, and gives high yields (>80%). RAIR is a useful technique that provides information about monolayer formation and also about the degree of

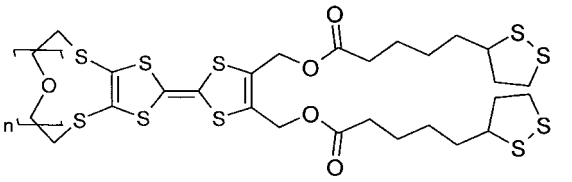

1: a (n=0), b (n=3), c (n=4), d (n=5)

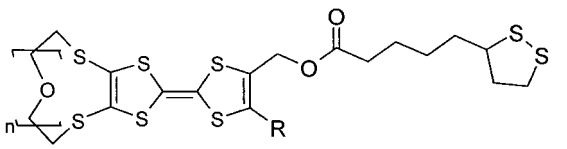

2: a (n=0, R=CO_2CH_3), b (n=5, R=H)

Fig. 3. New crown-ether annelated tetrathiafulvalene derivatives **1a**–**1d** and **2a** and **2b**.

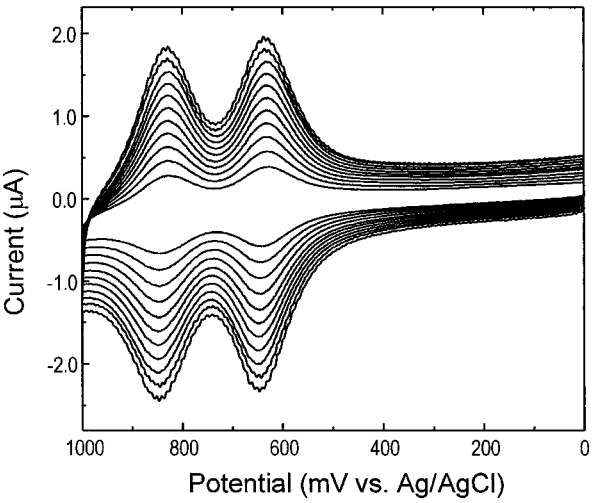

Fig. 4. CV analysis of the SAMs of **1b** in THF solution containing 0.1 M $TBAPF_6$ at different scan rates.

organization. For the conventional transmission spectrum of **1b** (used as reference, because the compounds are structurally very similar) along with those of the SAMs on a gold surface (see Table 1).

Comparison of the conventional transmission spectrum with those of the monolayers reveal, in the higher frequency region, a disorder or liquid-like packing around the environment of the methylene chains in the monolayer (almost the same wavelength) (48). Apparently, the increasing size of the appended crown results in more disordered monolayers. On the other hand, in the lower frequency range for the monolayer of **1b**, the —C═O, —C═C— and —C—O—C— stretchings are very weak, but the —C—S stretching at 666 cm^{-1} is very intense. These observations indicate that the two —C═O groups and the —C═C— are oriented almost parallel to the metal surface, whereas the —C—S part, from the crown, is more perpendicular. In contrast, the RAIR spectra of the monolayers of **1c** and **1d** show intense peaks for the —C═O and —C—O—C— stretching, but none is observed for the —C—S stretching, indicating that the orientation for the —C═O group in these structures is more perpendicular to the surface than in the case of **1b**.

Fig. 4 presents the variable scan rate dependence of the CVs for SAMs of **1b** on gold in a THF-electrolyte solution. Both TTF-based oxidations are clearly observed, and they are reversible. The observed peak current is proportional to the scan rate, indicating a surface-confined response (Fig. 4 and Table 2).

The anodic and cathodic peak-to-peak separations are less than 20 mV in all cases, and the full width at half-maximum is 95–110 mV in THF solution. Comparison with identical surface waves with zero peak-to-peak separation shows that these potential differences between the waves, which are independent of scan rate, are not caused by slow charge transfer kinetics (49, 50). For other surface-confined species this behavior has been explained on the basis of nonequilibrium states due to slow rate processes, such as electron transfer from the TTF redox center to the gold electrode via tunneling.

These SAMs are extremely stable, and their electrochemical responses remain essentially unchanged, specially for those of **1a**–**1d**. The latter exhibit almost the same current response even after more than 100 potential scan cycles. By far these are the most robust monolayers with which we have ever worked. The effect of adding alkali metal ions to these SAMs (Table 3) varied for the different compound-M^+ combinations.

As reported in homogeneous solution (28, 29), a significant anodic shift was observed for both the first and second redox processes of the SAMs of **1b**, **1c**, **1d**, and **2b** in THF solution when Na^+ was added. The largest anodic shift observed was for **1d**-Na^+ (60 mV). However, there is no potential shift observed for the SAMs of **1a** or **2a**, where no crown ether groups are present. These results indicate that the interaction of the metal ion with the dithia-crown ether must be responsible for the potential shifts. The recently published metal ion complexation studies of [60]fullerene derivatives of TTF-crown-ethers confirm this hypothesis (51). Although the C_{60}-based reduction potentials are not affected by metal ion complexation because of the long

Table 1. Vibrational mode assignment (cm^{-1}) of major peaks observed by transmission IR spectra of 1b and by RAIR spectroscopy of different TTF-based monolayers on a gold surface

Transmission IR of **1b**	RAIR of **1b**	RAIR of **1c**	RAIR of **1d**	Assignment
2,925	2,928	2,925	2,925	ν_{as}(—CH_2)
2,852	2,848	2,851	2,851	ν_a(—CH_2)
1,731	1,737	1,731	1,737	ν(—C═O)
1,540	1,571	—	—	ν(C═C) central
1,232	1,241	1,246	1,245	ν_{as}(—C—O—C—)
1,157	1,175	1,175	1,178	ν_s(—C—O—C—)
1,129	1,122	1,122	1,124	
974	—	946	950	
891	893	859	860	
783	—	740	744	ν(C—S) from TTF
731	—	—	—	
668	666	672	670	

Table 2. Electrochemical data of SAMs of the TTF disulfides in THF-$TBAPF_6$ system at room temperature with a scan rate of 100 mV·s^{-1}

SAMs of the disulfides	$E^1_{1/2}$ (ΔE_p)/mV	$E^2_{1/2}$ (ΔE_p)/mV
1a	654 (25)	904 (15)
1b	641 (12)	846 (5)
1c	661 (9)	841 (7)
1d	623 (20)	798 (15)
2a	719 (9)	996 (13)
2b	597 (7)	817 (7)

Table 3. Electrochemical shift for the SAMs of 1b–1d in the presence of different alkali metal ions (≈5 mM)

	SAMs of **1b**		SAMs of **1c**		SAMs of **1d**	
Metal ions	$E^1_{1/2}$	$E^2_{1/2}$	$E^1_{1/2}$	$E^2_{1/2}$	$E^1_{1/2}$	$E^2_{1/2}$
$LiPF_6$	0	0	0	0	0	0
$NaPF_6$	+10	0	+40	+35	+60	+55
KPF_6	0	0	+45	+38	+20	+30

distance between these centers, shifts were observed always for the TTF-centered oxidations, and these, as expected, were always anodic (more positive) (51).

The affinity sequence for the SAMs of **1b**, **1d**, and **1f** was $Na^+ > K^+ > Li^+$. However for **1c**, the order is $Na^+ \approx K^+ > Li^+$, similar to the solution behavior of the corresponding crown ethers (28, 29).

Bis-Thioctic Ester Derivatives of Oligo(ethyleneglycols) (OEG). After observing these cation recognition properties by the surface-confined crown-ether rings (19–24, 28, 29), we considered the idea of using glycols to form ion binding domains on the surface (similar to crown ethers) via the process of self-assembly. Ion recognition and sensing abilities by OEG-containing monolayers had not been explored at all until recently (30, 31).

Compounds **3-7** (Fig. 5) were easily synthesized, starting from the corresponding glycols and by reaction of these with thioctic acid in CH_2Cl_2 in the presence of dicyclohexylcarbodiimide (DCC) and 4-(dimethylamino) pyridine (DMAP) (30, 31). Compounds **3** and **4** were obtained from the same reaction as two separate products.

The monolayers prepared were characterized using reflection absorption infrared spectroscopy, cyclic voltammetry or impedance spectroscopy, reductive desorption, or by the determination of the double-layer capacitance.

The RAIR shows that the essential features are similar for all compounds studied, because they are structurally similar. The main peak assignments are shown in Table 4. In the higher-frequency region there are two absorption bands because of methylene stretching vibrations from both alkyl and OEG fragments. The peak positions of the respective methylene vibration bands in the mono-

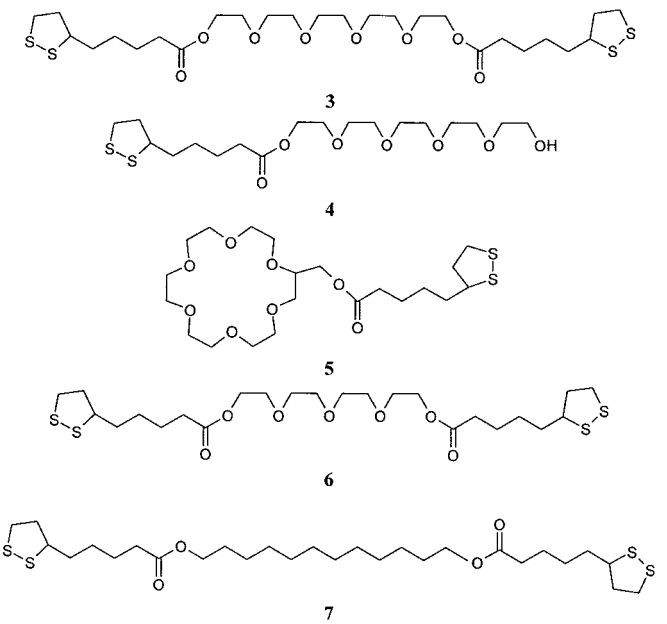

Fig. 5. Bis-thioctic ester derivatives of oligoethyleneglycols for SAMs formation.

Table 4. Vibrational mode assignment (cm^{-1}) of major peaks observed by RAIR spectroscopy of different OEG monolayers on gold surface

SAM of **3**	SAM of **5**	SAM of **6**	Assignment
2,925	2,924	2,925	$\nu_{as}(CH_2)$ alkyl unit
2,857	2,852	2,868	$\nu_s(CH_2)$ OEG unit
1,733	1,728	1,721	ν(—C═O)
1,454	1,454	1,449	CH_2-deformation
1,129	—	1,126	ν(C—O—C)
1,121	—	1,118	ν(C—O—C)
—	1,138	—	ν(—C—O) ether group
1,044	1,036	1,036	CH_2-rocking
948	949	948	

layer are almost the same when compared with the transmission spectra of the compounds, indicating that the alkyl chains in all of the monolayers are in a liquid-like disordered state (48). Analysis of the spectra in the lower frequency region shows a strong absorption band in the region of 1,740–1,721 cm^{-1} for the —C—O stretching of the carbonyl group (52). Furthermore, absorption bands between 1,126–1,129 cm^{-1} are attributed to the parallel polarized —C—O—C— stretching mode of the OEG part of the monolayer (53). Shoulders are also observed in the lower frequency region of the —C—O—C— stretching band at 1,118 cm^{-1} for **3** and 1,121 cm^{-1} for **6**, corresponding to the —C—O—C— stretching mode perpendicular to the OEG helical axis (54). Finally, a sharp peak was observed at 1,138 cm^{-1} for **5**, characteristic of the C—O stretching mode of the ether group (55).

Reductive desorption of the monolayer in 0.5 M KOH was used to estimate the surface coverage (56, 57). In all three cases an irreversible cathodic wave was observed at ≈ -0.9 V vs. Ag/AgCl, which corresponds to the surface attached thiolate groups. Integrating the current under the cathodic wave, and normalizing the results on the basis of the number of sulfurs presumably bonded to the surface, provides an estimated surface coverage of 6.2×10^{-11}, 4.6×10^{-11}, and 3.3×10^{-11} mol/cm^2 for **3**, **5**, and **6**, respectively. These values are lower than that observed for a thioctic acid (which is the anchoring segment for all of the compounds) monolayer on gold (58). The reduced surface coverage is partly due to the larger size and the presence of the two disulfide functionalities in **3** and **6**, and to the presence of the terminal crown ether group in **5**.

Cyclic voltammetry and impedance techniques allow the determination of the double-layer capacitance of these monolayers. The values obtained are between 11.2 and 16.4 $\mu F \cdot cm^{-2}$ in all cases. These values can be compared with the 25 $\mu F \cdot cm^{-2}$ for a bare gold electrode and the 8.5 $\mu F \cdot cm^{-2}$ for a thioctic acid monolayer (45). The results indicate that the monolayers are not densely packed, and that ions can easily permeate through them. CVs of $[Ru(NH_3)_6]^{3+/2+}$ (1 mM) in Et_4NCl (0.1 M) for monolayer modified gold electrodes of **3**, **5**, and **6** hardly show any influence on the heterogeneous electron transfer processes of the solution probe (peak currents and peak-to-peak separations for the couple at $E^\circ_{1/2} = -0.2$ V vs. Ag/AgCl remain essentially constant), providing additional evidence that the films are permeable to the redox active species.

The ion recognition at the interface of these structures was calculated by impedance spectroscopy, because none of the structural components of the SAMs are electroactive. Compound **7** forms a monolayer with an initial charge transfer resistance (R_{CT}) of 25 KΩ, but it exhibits no R_{CT} changes on exposure to either K^+ or Na^+. The mono ester compound **4** has almost no charge transfer blocking ability and behaves essentially as a bare gold electrode.

The more interesting results are for the monolayers constituted by **3** and **6**, which exhibit selective ion responses. The results are summarized in Fig. 6. Based on the graphs presented in Fig. 6 *a* and

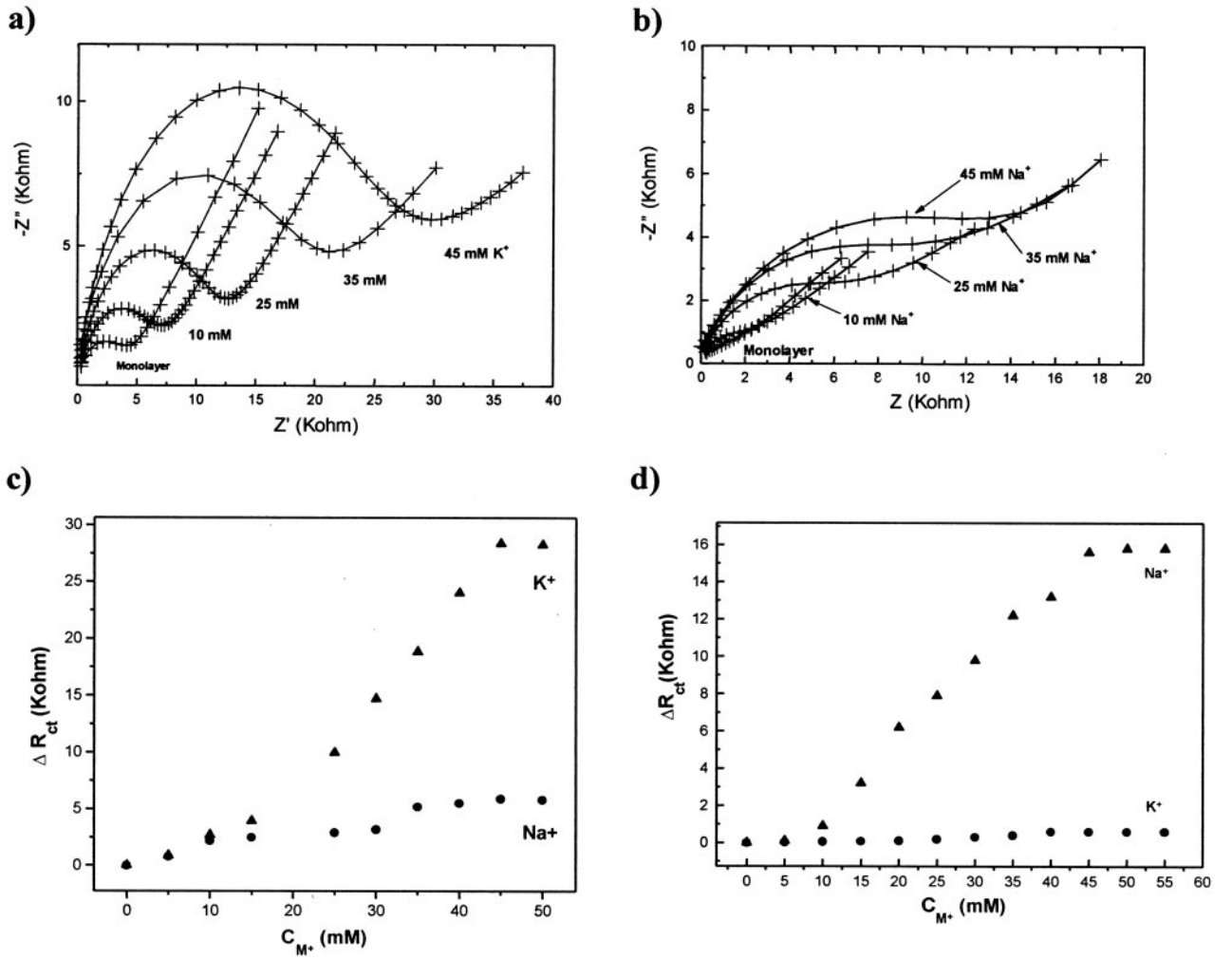

Fig. 6. (*a*) Impedance response of monolayer **3** in the absence and in the presence of varying amounts of [K^+]. (*b*) Impedance response of monolayer **6** in the absence and in the presence of varying amounts of [Na^+]. (*c*) Plot of the relative change of R_{CT} for **3** with [K^+] and [Na^+]. (*d*) Plot of the relative change of R_{CT} for **6** with [K^+] and [Na^+].

b, it is fair to say that a monolayer of **3** can act as a reversible and highly selective sensor for K^+ over Na^+ and in the case of the monolayer of **6** this selectivity is reversed. The selectivity for K^+ over Na^+ or vice versa suggests the formation of surface-confined pseudo18-crown-6 or pseudo15-crown-5 structures. This ion response selectivity can be easily observed from the plots of ΔR_{CT} vs. concentration for these ions as shown in Fig. 6 *c* and *d*. Assuming that the R_{CT} parameter is a direct measure of ion binding, the data can be fitted using a Langmuir isotherm. From this plot we have calculated the association constants for the different monolayers and metal ions (Table 5). Interestingly, the ion binding selectivity found for these structures is higher for the surface-confined podands when compared with those observed for the cyclic crown structures both in monolayers and in solution. To determine the

Table 5. Association constant (log K_a) of metal ions with different SAMs determined by fitting Langmuir model and calculated from changes of charge-transfer resistance

	SAM of **3**	SAM of **5**	SAM of **6**	18-crown-6*	15-crown-5*
K^+	2.82 (2.14)	3.25 (3.45)	1.26	2.03	0.76
Na^+	1.42	2.95	1.99 (1.79)	0.9	0.67

Quantitates inside the parentheses are association constant obtained by fitting a Langmuir model from a plot of θ vs. concentration of respective metal ion (see text).
*In aqueous solution (32).

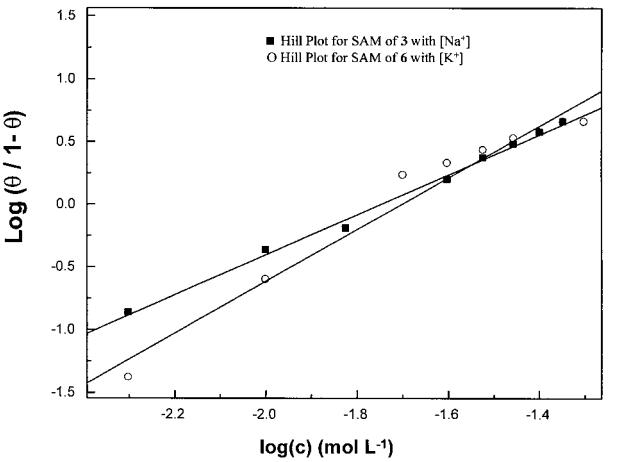

Fig. 7. Hill plots of monolayers **3** and **6** with [K^+] and [Na^+], respectively. The solid lines are the linear regressions of the respective data.

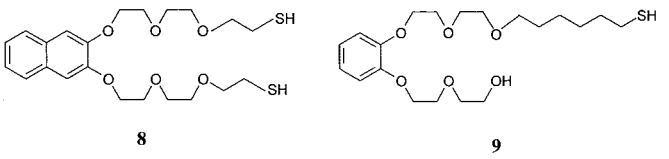

8 9

Fig. 8. Polyether derivatives with the capability of imprinting binding sites for potassium cations.

origin of the sigmoid binding curves for monolayers of **3** and **6**, the corresponding Hill plots were constructed (59), and are presented in Fig. 7. The Hill coefficients (η_H) determined from the slopes by linear regression were 1.7 and 2.1 for **3** and **6**, respectively, indicating positive cooperativity in the binding process for the two podands, possibly due to the reorganization of the monolayers on ion binding.

Ion-Imprinted SAMs for Ion Sensing. We have recently prepared new acyclic polyether thiol compounds that exhibit selective K^+ recognition if imprinted during SAM formation (structures **8** and **9** in Fig. 8).

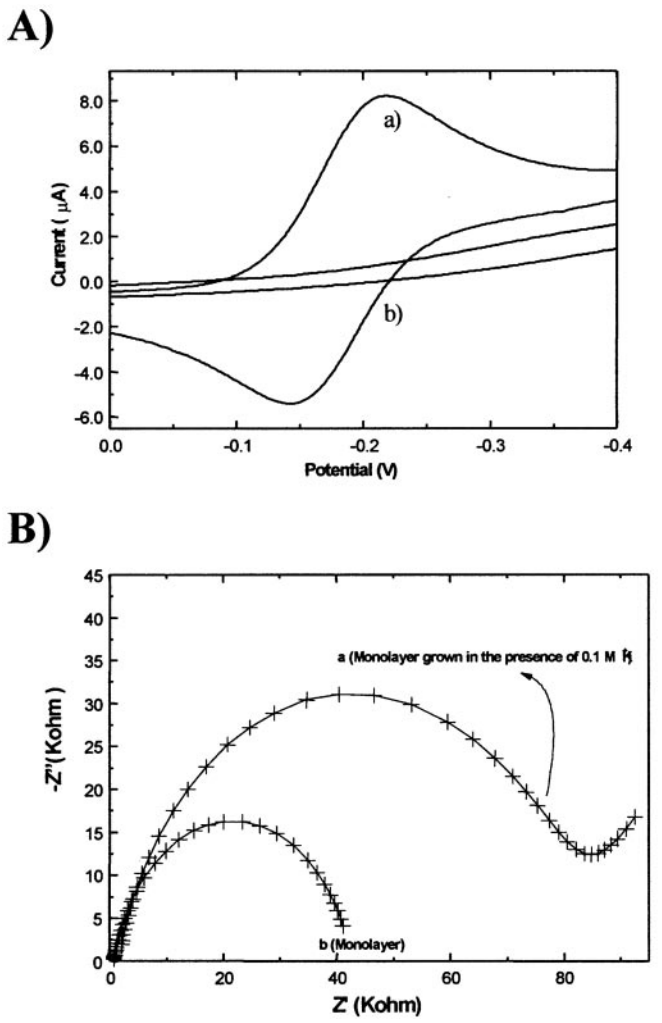

Fig. 9. (*A*) Cyclic voltammogram of 1 mM $Ru(NH_3)^{3+/2+}$ in 0.1 M tetraethylammonium chloride at (*a*) bare gold bead electrode and (*b*). Compound **8** modified gold bead electrode at a scan rate of 100 mV/s. (*B*) Complex impedance plot at dc bias of −0.20 V vs. Ag/AgCl in 1 mM $Ru(NH_3)^{3+/2+}$ in a 0.1 M aqueous solution of tetraethyl ammonium chloride for (*a*) monolayer of **8** grown in the presence of K^+ in solution and (*b*) monolayer grown without any K^+ in solution. The frequency range used was 1 KHz to 0.1 Hz with a 5-mV rms signal at ten steps per decade.

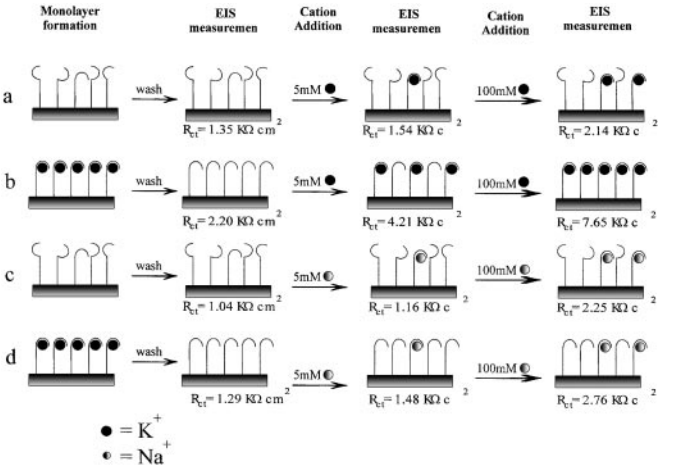

Fig. 10. Cartoon representation of the binding of metal cations by a SAM of 1 grown: (*a*) in the absence of KCl (*i*), and immersed in different $[K^+]$, (*b*) in the presence of 0.1M KCl (*ii*), and immersed in different $[K^+]$, (*c*) in the absence of KCl (*i*), and immersed in different $[Na^+]$, or (*d*) in the presence of 0.1M KCl (*ii*), and immersed in $[Na^+]$.

The quality of these SAMs was investigated by observing their effect on the voltammetric behavior of the $Ru(NH_3)_6^{3+/2+}$ couple present in solution. An almost complete disappearance of the Faradaic current was evident for the monolayer modified electrode as shown in Fig. 9*A*. The voltammetric features suggest that the SAM of compound **8** is capable of providing an effective barrier for electron transfer to the redox species in solution. Fig. 9*B* shows the impedance response of a monolayer of **8** grown on a gold electrode in the absence of K^+(curve b) and that of a monolayer of **8** grown in the presence of K^+ (curve a). The R_{CT} values obtained are 82.9 and 49.9 KΩ for parts a and b, respectively, indicating a reasonably effective blocking monolayer in both cases (60). The impedance response corresponding to the monolayer alone (b) contains no diffusional part. On the contrary, a small linear component is present in the lower frequency domain for the response of the monolayer grown in the presence of K^+, so the impedance data have been treated following two modified Randle's equivalent circuits (37). Rate constants were calculated to be 3.0×10^{-4} and 6.1×10^{-4} cm/s for the reactions in parts a and b of Fig. 9*B*, respectively. Although the decrease in the rate constants in both cases is 4 orders of magnitude relative to the rate constants of the redox couple at a bare gold electrode (>1 cm/s; ref. 61) the decrease is larger for the monolayer grown in the presence of K^+.

The different impedance experiments performed suggest the presence of two different binding states for K^+ in the surface-confined structure. The primary K^+ can be removed irreversibly and slowly in contrast to the second one, which exchanges reversibly and quickly. No K^+ incorporation occurs within preformed monolayers.

To probe the selectivity of this templating effect during SAM formation, monolayers were also grown in the presence of other metal ions (38). With $Ba^{2+}$and Ca^{2+}, the impedance responses are mostly dominated by diffusional components. Cs^+ shows some effects and is incorporated partially in the monolayer, whereas the presence of Na^+ has no effect and leads to an almost identical behavior to that of a simple monolayer. Definitely, the R_{CT} values in all of these cases are below that observed with K^+, indicating some selective templating during monolayer formation. RAIR spectroscopy suggested a more organized and oriented ethylene glycol helix in the monolayer of **8** grown in the presence of K^+. Based on the results obtained with **8**, receptor **9** was designed to be

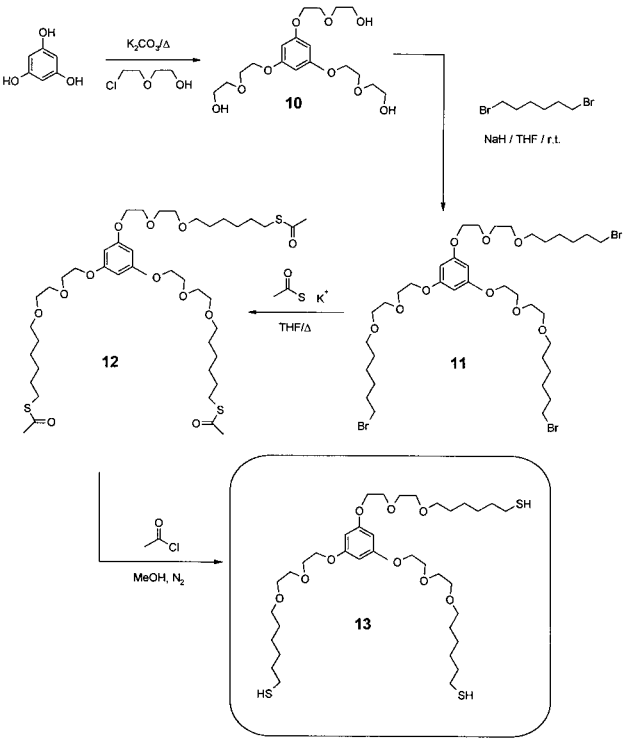

Scheme. 1. Different steps involved in the synthesis of the tripodal structure **13**.

used in a cation templating process on self-assembly on the gold surface.

Two kinds of SAMs were prepared using **9**, in the absence (*i*) or in the presence (*ii*) of K^+, and the charge-transfer resistances (R_{CT}) of both SAMs were measured in the presence of increasing concentrations of KCl. These results, as well as the ability of *i* and *ii* to recognize sodium cations are summarized in Fig. 10 (39). These results show that it is possible to imprint K^+ binding sites into SAMs when the monolayer is assembled on gold in the presence of this metal cation.

Ongoing efforts in this area have resulted in the design and synthesis of structures with three surface attachment groups (Scheme 1). Structure **13** has the potential to form surface-confined cryptate structures, which could be useful in the recognition of different cationic analytes.

Compound **13** was synthesized in four steps: reaction of 1,3,5-trihydroxybenzene with 2-chloroethoxyethanol afforded triol **10**, which was trialkylated with an excess of 1,6-dibromohexane (39). Treatment of this tribromoderivative with potassium thioacetate afforded the corresponding Tris(acetylthio) derivative **12** (62), which, after reaction with acetyl chloride in methanolic media, yielded the desired compound in quantitative amounts (the synthetic procedure will be reported elsewhere).

Conclusions

This article has presented the preparation and behavior of different surface-active compounds based on crown-ethers, oligoethylene glycols, or polyether derivatives. When incorporated as SAMs on gold these compounds are able to detect ion binding events on the surface. Because of the strong S–Au interactions, thiol, disulfide, and sulfide adsorbates were used as anchoring points for the formation of the SAMs.

The dithia-crown annelated TTFs compounds show well defined surface-confined redox waves, and their corresponding SAMs are extremely stable under a wide variety of conditions. The latter are able to recognize metal ions, and the process can be easily monitored following the potential shift of the TTF group, which can serve as a voltammetric sensor for electrochemically inactive ions.

SAMs prepared with the bis-thioctic ester podand derivatives show higher ion binding selectivities than those of analogous crown ethers. These glycols form ion recognition domains on gold that are surprisingly selective for ion sensing.

Finally, new semirigid structures with ethylene glycol arms selectively detect potassium cations when their SAMs are imprinted in their presence. The concept of ion-imprinted SAMs for sensing application shows considerable promise. Judicious choice of structures with various degrees of rigidity and preorganization could result in selective and sensitive systems for ion sensing.

We wish to express our gratitude to the Chemistry Division of the National Science Foundation (CHE-9816503) for generous financial support. We also want to thank some of the members of our group who initiated this area of research: Dr. K. Bandyopadhyay, Dr. H. Liu, Dr. S. G. Liu, and Dr. L. Shu. Special thanks to Dr. L. E. Echegoyen for her editing assistance in the final stages of the manuscript.

1. Nuzzo, R. G. & Allara, D. L. (1983) *J. Am. Chem. Soc.* **120,** 4481–4483.
2. Lehn, J. M. (1988) *Angew. Chem. Int. Ed. Engl.* **27,** 89–112.
3. Lehn, J. M. (1993) *Science* **260,** 1762–1763.
4. Haüssling, L., Ringsdorf, H., Schmitt, E.-J. & Knoll, W. (1991) *Langmuir* **7,** 1837–1840.
5. Philp, D. & Stoddart, J. F. (1996) *Angew. Chem. Int. Ed. Engl.* **35,** 1155–1196.
6. Zhang, L., Zou, B., Dang, D., Huo, F. W., Zhang, X., Chi, L. F. & Jiang, L. (2001) *Chem. Commun.*1906–1907.
7. Kondo, T., Kanou, T. & Uosaki, K. (2001) *Langmuir* **17,** 6317–6324.
8. Lahav, M., Kharitonov, A. B. & Willner, I. (2001) *Chem. Eur. J.* **7,** 3992–3997.
9. Crego-Calama, M. & Reinhoudt, D. N. (2001) *Adv. Mater.* **13,** 1171–1174.
10. Rubinstein, I., Steinberg, S., Tor, Y., Shanzer, H. & Sajiv, J. (1988) *Nature (London)* **332,** 426–429.
11. Steinberg, S., Tor, Y., Sabatani, E. & Rubinstein, I. (1991) *J. Am. Chem. Soc.* **113,** 5176–5182.
12. Rojas, T. M., Königer, R., Stoddart, J. F. & Kaifer, A. E. (1995) *J. Am. Chem. Soc.* **117,** 336–343.
13. Henke, C., Steinem, C., Janshoff, A., Steffan, G., Luftmann, H., Sieber, M. & Galla, H.-J. (1996) *Anal. Chem.* **68,** 3158–3165.
14. Friggeri, A., van Veggel, F. C. J. M. & Reinhoudt, D. N. (1998) *Langmuir* **14,** 5457–5463.
15. Huisman, B.-H., Rudkevich, D. M. J., van Veggel, F. C. J. M. & Reinhoudt, D. N. (1996) *J. Am. Chem. Soc.* **118,** 3523–3524.
16. Huisman, B.-H., Thoden van Velzen, E. U., van Veggel, F. C. J. M., Engbersen, J. F. J. & Reinhoudt, D. N. (1995) *Tetrahedron Lett.* **36,** 3273–3276.
17. Arias, F., Godínez, L. A., Wilson, S. R., Kaifer, A. E. & Echegoyen, L. (1996) *J. Am. Chem. Soc.* **118,** 6086–6087.
18. Miura, Y., Kimura, S., Imanishi, Y. & Umemura, J. (1998) *Langmuir* **14,** 2761–2767.
19. Flink, S., Boukamp, B. A., van der Berg, A., van Veggel, F. C. J. M. & Reinhoudt, D. N. (1998) *J. Am. Chem. Soc.* **120,** 4652–4657.
20. Flink, S., van Veggel, C. J. M. & Reinhoudt, D. N. (1999) *J. Phys. Chem. B* **103,** 6515–6520.
21. Van der Veen, N. J., Flink, S., Deij, M. A., Egberink, R. J. M., van Veggel, F. C. J. M. & Reinhoudt, D. N. (2000) *J. Am. Chem. Soc.* **122,** 6112–6113.
22. Flink, S., Sconherr, H., Vancso, G. J., Geurts, F. A. J., van Leerdam, K. G. C., van Veggel, F. C. J. M. & Reinhoudt, D. N. (2000) *J. Chem. Soc. Perkin Trans 2* 2141–2146.
23. Moore, A. J., Goldenberg, L. M., Bryce, M. R., Petty, M. C., Monkman, P., Marenco, C., Yarwood, J., Joyce, M. J. & Port, S. N. (1998) *Adv. Mater.* **10,** 395–398.
24. Moore, A. J., Goldenberg, L. M., Bryce, M. R., Petty, M. C., Moloney, J., Howard, J. A. K., Joyce, M. J. & Port, S. N. (2000) *J. Org. Chem.* **65,** 8269–8276.
25. Gafni, Y., Weizman, H., Libman, J., Shanzer, A. & Rubinstein, I. (1996) *Chem. Eur. J.* **2,** 759–766.
26. Stora, T., Hovious, R., Dienes, Z., Pachoud, M. & Vogel, H. (1997) *Langmuir* **13,** 5211–5214.
27. Rudkevich, D. M. (2000) *Chem. Eur. J.* **6,** 2679–2686.
28. Liu, H., Liu, S.-G. & Echegoyen, L. (1999) *Chem. Commun.* 1493–1494.
29. Liu, S.-G., Liu, H., Bandyopadhyay, K., Gao, Z. & Echegoyen, L. (2000) *J. Org. Chem.* **65,** 3292–3298.
30. Bandyopadhyay, K., Liu, H., Liu, S.-G. & Echegoyen, L. (2000) *Chem. Commun.*141–142.

31. Bandyopadhyay, K., Liu, S.-G., Liu, H. & Echegoyen, L. (2000) *Chem. Eur. J.* **6,** 4385–4392.
32. Izatt, R. M., Pawlak, K. & Bradshaw, J. S. (1995) *Chem. Rev.* **95,** 2529–2586.
33. Haupt, K. & Mosbach, K. (2000) *Chem. Rev.* **100,** 2495–2504.
34. Chailapakul, O. & Crooks, R. M. (1993) *Langmuir* **9,** 884–888.
35. Chailapakul, O. & Crooks, R. M. (1995) *Langmuir* **11,** 1329–1340.
36. Lahav, M., Katz, E., Doron, A., Patolsky, F. & Willner, I. (1999) *J. Am. Chem. Soc.* **121,** 862–863.
37. Mirsky, V. M., Hirsch, T., Piletsky, S. A. & Wolfbeis, O. S. (1999) *Angew. Chem. Int. Ed. Engl.* **8,** 1108–1110.
38. Bandyopadhyay, K., Shu, L., Liu, H. & Echegoyen, L. (2000) *Langmuir* **16,** 2706–2714.
39. Colonna, B. & Echegoyen, L. (2001) *Chem. Commun.* 1104–1105.
40. Gómez, M. E., Li, J. & Kaifer, A. E. (1991) *Langmuir* **7,** 1797–1806.
41. Goss, C. A., Charych, D. H. & Majda, M. (1991) *Anal. Chem.* **63,** 85–88.
42. Boukamp, B. A. (1986) *Solid State Ionics* **20,** 31–44.
43. Fujihara, I., Nakai, H., Yoshihara, M. & Maeshima, T. (1999) *Chem. Commun.* 737–738.
44. Shon, Y.-S. & Lee, T. R. (1999) *Langmuir* **15,** 1136–1140.
45. Cheng, Q. & Brajter-Toth, A. (1992) *Anal. Chem.* **64,** 1998–2001.
46. Fibbioli, M., Bandyopahhyay, K., Liu, S.-G., Echegoyen, L., Enger, O., Diederich, F., Bühlmann, P. & Prestch, E. (2000) *Chem. Commun.* 339–340.
47. Blanchard, P., Sallé, M., Duguay, G., Jubault, M. & Gorgues, A. (1992) *Tetrahedron Lett.* **33,** 2685–2688.
48. Seshadri, K., Atre, S. V., Tao, Y. T. & Lee, M. T. (1997) *J. Am. Chem. Soc.* **119,** 4698–4711.
49. Chidsey, C. E. D. (1991) *Science* **251,** 919–922.
50. Feldberg, S. W. & Rubinstein, I. (1988) *J. Electroanal. Chem.* **240,** 1–15.
51. Liu, S.-G. & Echegoyen, L. (2000) *Eur. J. Org. Chem.* 1157–1163.
52. Socrates, G. (1994) *Infrared Characteristic Group Frequencies* (Wiley, New York).
53. Pertsin, A. J., Grunze, M. & Garbuzova, I. A. (1998) *J. Phys. Chem.* **102,** 4918–4926.
54. Miyazawa, T., Fukushima, K. & Ideguchi, Y. (1962) *J. Chem. Phys.* **37,** 2764–2769.
55. Bruening, M. L., Zhou, Y., Aguilar, G., Agee, R., Bergbreiter, D. E. & Crooks, R. M. (1997) *Langmuir* **13,** 770–778.
56. Walczak, M. M., Popenoe, D. D., Deinhammer, R. S., Lamp, B. D., Chung, C. & Porter, M. D. (1991) *Langmuir* **7,** 2687–2693.
57. Weisshaar, D. E., Lamp, B. D. & Porter, M. D. (1992) *J. Am. Chem. Soc.* **114,** 5860–5862.
58. Wang, Y. & Kaifer, A. E. (1998) *J. Phys. Chem. B* **102,** 9922–9927.
59. Fitzmaurice, D., Rao, S. N., Preece, J. A., Stoddart, J. F., Wenger, S. & Zaccheroni, N. (1999) *Angew. Chem. Int. Ed. Engl.* **38,** 1147–1150.
60. Lukkari, J., Meretoja, M., Kartio, I., Laajalehto, K., Rajamäki, M., Lindström, M. & Kankar, J. (1999) *Langmuir* **15,** 3529–3537.
61. Endicott, J. F., Scroeder, R. X., Chidester, D. H. & Ferrier, D. R. (1973) *J. Phys. Chem.* **77,** 2579–2583.
62. Gittins, D. I., Bethell, D., Nichols, R. J. & Schiffrin, D. J. (2000) *J. Mater. Chem.* **10,** 79–83.